S 26948: a New Specific Peroxisome Proliferator–Activated Receptor γ Modulator With Potent Antidiabetes and Antiatherogenic Effects

Maria Carmen Carmona,[1] Katie Louche,[1] Bruno Lefebvre,[2] Antoine Pilon,[3] Nathalie Hennuyer,[3] Véronique Audinot-Bouchez,[4] Catherine Fievet,[3] Gérard Torpier,[3] Pierre Formstecher,[2] Pierre Renard,[5] Philippe Lefebvre,[2] Catherine Dacquet,[5] Bart Staels,[3] Louis Casteilla,[1] and Luc Pénicaud[1] on behalf of the Consortium of the French Ministry of Research and Technology

OBJECTIVE—Rosiglitazone displays powerful antidiabetes benefits but is associated with increased body weight and adipogenesis. Keeping in mind the concept of selective peroxisome proliferator–activated receptor (PPAR)γ modulator, the aim of this study was to characterize the properties of a new PPARγ ligand, S 26948, with special attention in body-weight gain.

RESEARCH DESIGN AND METHODS—We used transient transfection and binding assays to characterized the binding characteristics of S 26948 and GST pull-down experiments to investigate its pattern of coactivator recruitment compared with rosiglitazone. We also assessed its adipogenic capacity in vitro using the 3T3-F442A cell line and its in vivo effects in *ob/ob* mice (for antidiabetes and antiobesity properties), as well as the homozygous human apolipoprotein E2 knockin mice (E2-KI) (for antiatherogenic capacity).

RESULTS—S 26948 displayed pharmacological features of a high selective ligand for PPARγ with low potency in promoting adipocyte differentiation. It also displayed a different coactivator recruitment profile compared with rosiglitazone, being unable to recruit DRIP205 or PPARγ coactivator-1α. In vivo experiments showed that S 26948 was as efficient in ameliorating glucose and lipid homeostasis as rosiglitazone, but it did not increase body and white adipose tissue weights and improved lipid oxidation in liver. In addition, S 26948 represented one of the few molecules of the PPARγ ligand class able to decrease atherosclerotic lesions.

CONCLUSIONS—These findings establish S 26948 as a selective PPARγ ligand with distinctive coactivator recruitment and gene expression profile, reduced adipogenic effect, and improved biological responses in vivo. ***Diabetes*** **56:2797–2808, 2007**

From the [1]UMR 5241, UPS-CNRS, IFR 31, BP84225, Toulouse, France; the [2]U459 INSERM, Lille, France; the [3]U545 INSERM, Département d'Athérosclérose, Institut Pasteur de Lille and University of Pharmacy Lille II, Lille, France; the [4]Division of Molecular and Cellular Pharmacology, Institut de Recherche Servier, Croissy sur Seine, France; and the [5]Division of Experimental Therapeutic and Division of External Chemistry, Institut de Recherches Internationales Servier, Courbevoie, France.

Address correspondence and reprint requests to Luc Pénicaud, UMR 5241 CNRS-UPS, IFR 31, BP84225, 31432 Toulouse Cedex 4, France. E-mail: penicaud@toulouse.inserm.fr.

Received for publication 14 December 2006 and accepted in revised form 10 August 2007.

Published ahead of print at http://diabetes.diabetesjournals.org on 17 August 2007. DOI: 10.2337/db06-1734.

Apo, apolipoprotein; DMEM, Dulbecco's modified Eagle's medium; FFA, free fatty acid; IDL, intermediate-density lipoprotein; iWAT, inguinal white adipose tissue; NEFA, nonesterified fatty acid; PGC, peroxisome proliferator–activated receptor γ coactivator; PPAR, peroxisome proliferator–activated receptor; RXR, retinoic X receptor; SPPARM, selective PPARγ modulator; TNF, tumor necrosis factor; TZD, thiazolidinedione; UCP, uncoupled protein; WAT, white adipose tissue.

The peroxisome proliferator–activated receptors (PPARs) (1) are transcription factors belonging to the nuclear receptor transcription factor family (1). Three isoforms, PPARα, -δ, and -γ, have been described to have tissue-specific patterns of expression and function—the latter being highly expressed in adipocytes and macrophages among other cell types (2–5). The role of PPARγ on adipocyte differentiation has been extensively studied in vitro and in vivo (2,3,6,7). Forced expression of PPARγ in nonadipogenic cells is sufficient to induce adipocyte differentiation on treatment with specific agonists (6,8). On the other hand, loss-of-function experiments demonstrated the absolute requirement of PPARγ for adipose terminal differentiation (6,7). In macrophages, PPARγ controls cytokine production and intracellular cholesterol trafficking and efflux (9,10), thus reducing lipid accumulation and atherosclerotic lesions (9,11).

PPARγ heterodimerizes with the retinoic X receptor (RXR)α (2). Ligand binding to its receptor induces specific conformational changes that allow the release of corepressors and the binding of coactivators to the PPARγ-RXRα heterodimer. According to the model proposed by Olefsky (12) and Sporn et al. (13), each ligand-receptor complex adopts a different three-dimensional conformation, leading to distinct interactions with cofactors and other transcription factors. As a consequence, each PPARγ ligand activates differential but overlapping patterns of functions. This model of selective PPARγ modulator (SPPARM) may explain the different pattern of activation of gene expression observed between different PPARγ ligands.

Natural (14–18) and synthetic (19–27) ligands for PPARγ are lipid-derived compounds that bind to and transactivate the receptor with distinct affinities. Among those, the thiazolidinedione (TZD) class of drugs is currently used for the treatment of type 2 diabetes (28). They normalize glycemia and decrease insulin as well as free fatty acid serum levels in type 2 diabetic rodents and human subjects (29,30) and reduce atherosclerosis in certain mouse models (11).

Among the adverse side effects of TZD treatment, the tendency to cause body-weight gain in rodents and in humans, in part due to increasing fat mass, has been very extensively characterized (31–34). In the past few years, there has been a considerable effort in identifying antidiabetes drugs capable of exerting their effects without affecting body weight, but most compounds developed thus far do not overcome this adverse effect (28,35,36).

In this study, we identify and analyze a novel non-TZD drug, S 26948, a high-affinity ligand for PPARγ (37). The binding of S 26948 to PPARγ induces a different pattern of coactivator recruitment compared with rosiglitazone, a commonly used TZD. This new SPPARM has powerful antidiabetes and antiatherogenic effects without proadipogenic properties.

RESEARCH DESIGN AND METHODS

Chemicals. The compound S 26948, Servier, a racemate of dimethyl-2-{4-[2-(6-benzoyl-2-oxo-1,3-benzothiazol-3(2H)yl)ethoxy]benzyl}malonate (37), was synthetized at the Pharmaceutical Chemistry Institute, EA 1043, Faculty of Pharmacy of Lille (Prof. D. Lesieur). The reference compound (rosiglitazone) was obtained from the same source. Both compounds were solved in 10 mmol/l DMSO.

Construction of recombinant plasmids. Plasmids pGal4-hPPARγ, pGal4-hPPARα, pGal4-hPPARδ, and pG5-TK-pGL3 were constructed as previously described (38).

Transient transfection assays. Cos-7 cells were seeded in 60-mm dishes at a density of 5.5×10^5 cells/dish in Dulbecco's modified Eagle's medium (DMEM) supplemented with 10% FCS and incubated at 37°C for 24 h before transfection. Cells were transfected in OptiMEM without FCS for 3 h at 37°C, using polyethylenimine, with reporter and expression plasmids, as stated in the figure legends. The plasmid pBluescript (Stratagene, La Jolla, CA) was used as carrier DNA to set the final amount of DNA to 5.5 μg/dish. The pCMV-β-galactosidase expression plasmid was cotransfected as a control for transfection efficiency. Transfection was stopped by the addition of DMEM supplemented with 10% FCS, and cells were then incubated at 37°C. After 16 h, cells were trypsinized and seeded in 96-well plates at the density of 2×10^4 cells/well and incubated for 6 h in 10% FCS–containing DMEM. Cells were then incubated for 24 h in DMEM containing 0.2% FCS and increasing concentrations of the compound tested or vehicle (DMSO). At the end of the experiment, cells were washed once with ice-cold PBS, and the luciferase and β-galactosidase assays were performed as previously described (39). Half-maximal effective concentration (EC_{50}) was estimated using Prism software (GraphPad). All transfection experiments were performed at least three times.

Membrane-bound PPARγ binding assay. Binding assays, using a human full-length PPARγ construct expressed in bacteria, were performed in 96-well plates. Binding buffer consisted of 10 mmol/l Tris/HCl, pH 8.2, 50 mmol/l KCl, and 1 mmol/l dithiothreitol. Membrane preparations (5 μg/ml) were incubated for 180 min at 4°C in the presence of [^{3}H]rosiglitazone (BRL49653; Amersham Biosciences) (10 nmol/l) and the tested compounds. Nonspecific binding was defined using an excess of unlabeled rosiglitazone (10 μmol/l). Incubation was terminated by the addition of ice-cold 50 mmol/l Tris/HCl buffer, pH 7.4, followed by rapid filtration under reduced pressure through Whatman GF/C filter plates presoaked with ice-cold buffer, followed by three successive washes with the same buffer. Radioactivity was measured in a Top-count apparatus (Packard).

K_i values were calculated according to the equation $K_i = IC_{50}/\{1 + ([L]/K_d)\}$, where IC_{50} is the concentration of test compound required to inhibit 50% of the specific binding of the radioligand, [L] is the concentration of the radioligand used, and K_d is the dissociation constant for the radioligand at the receptor (40). Each experiment was performed twice, and points were in triplicate.

Cell culture. 3T3-F442A preadipocytes were cultured in DMEM supplemented with 10% FCS and 1% antibiotics (streptomycin, penicillin, and amphotericyn). Cells were grown to confluence and treated with the same volume of solvent (10 mmol/l DMSO, control cells), rosiglitazone (0.01–10 μmol/l), or S 26948 (0.01–10 μmol/l) every 2 days. Adipogenesis was determined by Oil red O staining or triglyceride quantification using the Triglycerides Enzymatic PAP150 kit from BioMérieux (Marcy-l'Etoile, France), and the expression of adipocyte-specific mRNA markers was measured. Protein content was determined using the DC Protein Assay system from Bio-Rad Laboratories (Hercules, CA).

GST pull-down experiments. The protocol used has been published elsewhere with minor modifications (41,42). In a typical binding reaction, 5–10 pmol of in vitro translated ^{35}S-PPARγ (TnT system; Promega) was incubated with DMSO or ligand (10 μmol/l) in 20 mmol/l Tris-HCl (pH 7.5), 150 mmol/l NaCl, 10% glycerol, and 0.1% Triton X-100. Both isoforms (PPARγ_2 and -γ_1) were obtained by coupled transcription/translation, since the cDNA coding for the -γ_2 isoform contains all the sequences necessary for -γ_1 translation. The presence of both isoforms is very likely to result from the alternative use of start codon on the transcribed PPARγ_2 cDNA.

After 60 min incubation at 20°C (200 μl final volume), 40 μl of a 50% Sepharose-glutathione GST-coactivator slurry was added to the mix and agitated slowly on a rotating wheel for 90 min at 20°C. Unbound material was removed by three successive washes of the Sepharose beads by 10 vol of 1× PBS–0.1% Triton X100. Resin-bound receptors were then resolved by 10% SDS-PAGE and detected and quantified by autoradiography on a PhosphorImager (Molecular Dynamics). All assays were performed at least in triplicate with distinct coactivator extracts.

Yeast two-hybrid assays. The assay was based on interaction mating using the Clontech Matchmaker Two Hybrid System 3. Briefly, full-length PPARγ was expressed as a Gal4-DBD fusion protein (pGBT9 vector; Clontech) and transformed into the AH109a yeast strain; the coactivator or corepressor receptor–interacting domain was inserted into the pGAD24 vector to generate a fusion protein with the Gal4 activation domain (DRIP205: amino acid 459–803, PPARγ coactivator [PGC]1: 190–403, SRC1: 459–888, CBP: 8–93, GRIP1: 548–878, and SMRT: 373-1191). After mating, the diploid cells were subjected to two rounds of replication and selected for interacting clones. A fluorogenic substrate was used to quantify the interaction at various ligand concentrations (10 different concentrations, ranging from 50 nmol/l to 50 μmol/l). Results were expressed in fluorescence units as the difference between "no cofactor" control experiments and the signal obtained in cofactor PPARγ studies. Areas under the curve were calculated and plotted as bar graphs. All experiments were carried out at Phenex, Germany.

Animals and treatment. The care and use of mice were in accordance with the European Community Council Directive 86/609/EEC and approved by the Comité d'Ethique et d'Expérimentation Animale of the University Paul Sabatier (Toulouse, France) and Institut Pasteur (Lille, France). Obese (*ob/ob*) male C57BL/6 mice were kept under standard conditions of housing (12-h light/dark cycles), feeding (diet: UAR, Villemoissson sur Orge, France; food and water ad libitum), and environment temperature (21°C). Mice were randomly divided into three groups (vehicle control: DMSO 10%/solutol HS 15 [BASF] 15% and sterile water 75% [vol/vol/vol], 10 mg/kg rosiglitazone, and 30 mg/kg S 26948; $n = 5–6$ animals per group) and injected intraperitonealy once daily (5 ml/kg). Body weight and food intake were measured daily. After 13 days of treatment, mice were killed by decapitation after CO_2 anesthesia and blood samples collected for immediate assessment of glucose levels. Plasma was frozen for posterior metabolite quantification.

Homozygous human apolipoprotein (apo)E2 knockin mice (E2-KI) mice were used in the atherosclerotic lesion study. These mice express human apoE2 instead of mouse apoE (43). Male mice ($n = 9–10$ per group) were fed a Western diet containing (wt/wt) 0.2% cholesterol and 21% fat (UAR, Epinay sur Orge, France) supplemented without (control group) or with rosiglitazone (10 mg/kg) or S 26948 (30 mg/kg) for 9 weeks. The mice had ad libitum access to water. Blood was collected after a 6-h fasting period by sinus retroorbital puncture under isoflurane-induced anesthesia for biochemical analysis.

Metabolite measurements. Blood glucose levels were measured using Glucotrend and Accu-Check active systems (Roche, Mannheim, Germany). Plasma nonesterified fatty acid (NEFA) was determined using an acyl-CoA oxidase–based colorimetric kit (NEFA-C; Wako Pure Chemicals, Neuss, Germany). Plasma triglycerides were measured using enzymatic colorimetric methods (Triglycerides Enzymatic PAP150; BioMérieux, Marcy-l'Etoile, France). Serum insulin levels were determined by an immunoassay enzymatic system (Mercodia Ultrasensitive Mouse Insulin ELISA; Mercodia, Uppsala, Sweden). Plasma levels of total cholesterol were measured using commercially available kits (Boehringer). HDL cholesterol concentrations were determined after precipitation of apoB-containing lipoproteins with phosphotungstic acid per milligram (Boehringer). Non-HDL cholesterol values were calculated by substracting HDL cholesterol from total cholesterol.

Lipoprotein cholesterol and triglycerides distribution profiles were obtained by gel filtration chromatography using a superose 6 HR 10/30 column (Amersham Pharmacia Biotech) on pooled plasma samples from each group.

Real-time PCR. Total RNA from cultured cells or frozen tissues was extracted using the Extract-all solution (Eurobio). Complementary DNA was synthesized with the Super ScriptTM reverse transcriptase and poly dT primers (Invitrogen). The real-time PCR measurement of individual cDNAs was performed using SYBR Green dye to measure duplex DNA formation with the Gene Amp 5700 (Applied Biosystem) and normalized to the amount of cyclophilin RNA. The following primers were used: adiponectin forward TCCTGGAGAGAAGGGAGAGAAAG, reverse CCCTTCAGCTCCTGTCATTCC; aP2 forward GATGCCTTTGTGGGAACCTG, reverse GCCATGCCTGCCA CTTTC; CCAAT/enhancer-binding protein α forward GAGCCGAGATAAAGC CAAACA, reverse GCGCAGGCGGTCATTG; Cyclophilin forward GATG AGAACTTCATCCTAAAGCATACA, reverse TCAGTCTTGGCAGTGCAGATAA A; LPL forward GTGGCCGAGAGCGAGAAC, reverse CCACCTCCGTGTA AATCAAGAAG; PEPCK forward GCCACAGCTGCTCGCAGAA, reverse GAA GGGTCGCATGGCAAA; PPARγ_2 forward AGTGTGAATTACAGCAAATCTC TGTTTT, reverse GCACCATGCTCTGGGTCAA; and tumor necrosis factor (TNF)α forward GCAGTCTGTGTCTGCTGGGAT, reverse CGCAGAACGG GATGAAGC.

Histological analysis and immunohystochemistry. Adipose tissue specimens were fixed in 95% ethanol overnight for histological analysis and embedded in paraffin. Sections were cut at a thickness of 5 μm and stained with hemalun/eosin. Inguinal white adipose tissue (iWAT) sections were incubated for 1 h at room temperature with 0.5 μg/ml uncoupled protein (UCP)11-A. Second antibody coupled to alkaline phosphatase (1:200) was visualized using BCIP/NBT. Endogenous alkaline phosphatase activity was inhibited by levamisole. Control experiments were performed using purified rabbit IgG. Adipocyte size and distribution were determined by the vertical sections method (44,45).

Fatty acid oxidation in liver. Palmitate oxidation rates were measured in liver homogenates as previously described (46). Small fragments of liver were homogenized in Set buffer (250 mmol/l sucrose, 2 mmol/l EDTA, and 10 mmol/l Tris, pH 7.4), and 75 μl were incubated in 300 μl of oxidation buffer (27 mmol/l KCl, 10 mmol/l KH_2PO_4, 5 mmol/l $MgCl_2$, 1 mmol/l EDTA, 25 mmol/l sucrose, 75 mmol/l Tris, 5 mmol/l ATP, 1 mmol/l NAD^+, 25 μmol/l cytochrome *c*, 0.1 mmol/l coenzyme A, 0.5 mmol/l L-carnitine, and 0.5 mmol/l L-malate, pH7.4) in glass vials. After a 5-min preincubation at 37°C in a shaking-water bath, the reaction was started by adding 100 μl of 600 μmol/l [1-^{14}C]palmitic acid (Amersham Pharmacia Biotech, Orsay, France) bound to fatty acid–free BSA in a 5:1 molar ratio. Incubation was carried out for 30 min and stopped by adding 200 μl of 3M perchloric acid. The $^{14}CO_2$ produced was trapped in 300 μl ethanolamine/ethylene glycol (1:2 vol/vol) and measured using a liquid scintillation counter. After 90 min at 4°C, the acid incubation mixture was centrifuged (5 min at 10,000*g*), and 500 μl of supernatant containing the ^{14}C-perchloric acid acid-soluble products was assayed for radioactivity by liquid scintillation. Palmitate oxidation rates were calculated from the sum of $^{14}CO_2$ and ^{14}C-percholic acid-soluble products and expressed in nanomoles of palmitate per minute per gram tissue weight or picomoles of palmitate per minute per milligram of protein.

Analysis of atherosclerotic lesions. Mice were killed by cervical dislocation; the heart of each animal was fixed with 4% phosphate-buffered paraformaldehyde (pH 7.0), and serial 10-μm-thick sections were cut between the valves and the aortic arch for quantitative analysis of lipid deposition by Oil red O. Images were captured by use of a JVC 3-charge-coupled device video camera. Sections were analyzed using the computer-assisted Quips Image analysis system (Leica Mikroskopic und System, Wetzlar, Germany).

Statistical analysis. Data are expressed as means ± SE. Prism Software (GraphPad, San Diego, CA) was used for all statistical analysis. A one-way ANOVA followed by Tukey's multiple comparison test was used to assess the statistical difference between groups. When appropriate, an unpaired *t* test was performed.

RESULTS

S 26948 is a specific high-affinity agonist for PPARγ. To examine whether S 26948 activated PPARγ, we used a transient transfection reporter assay in COS-7 cells. S 26948 was unable to significantly activate RXRα (Fig. 1*A*), human PPARα (Fig. 1*B*), and PPARβ/δ (Fig. 1*C*) at concentrations up to 10 μmol/l. By contrast, it strongly activated human PPARγ in a dose-dependent manner using chimeric protein construct (Fig. 1*D*) or using full-length construct cotransfected with RXRα (Fig. 1*E*). The EC_{50} for S 26948 was not significantly different from rosiglitazone (Fig. 1*D* and *E*). Furthermore, in a binding assay using [^{3}H]rosiglitazone and hPPAR-LBD (45), S 26948 bound PPARγ with the same affinity as rosiglitazone (Fig. 1*F*); K_i values were not significantly different.

Differential effects of S 26948 and rosiglitazone on adipocyte differentiation. 3T3-F442A cells were grown to differentiate in the absence or presence of various concentrations of S 26948 or rosiglitazone. As an index of differentiation, the triglyceride content per milligram protein of the cells was assessed (Fig. 2*A*). As expected, rosiglitazone significantly increased the triglyceride content in a dose-dependent manner after 8 days of treatment compared with control values ($P < 0.001$). By contrast, S 26948 did not increase the triglyceride content of the cells at any concentration tested. Microscopic observation of the cell culture showed that at the end of the differentiation (day 8), cells treated with 100 nmol/l S 26948 had morphologic features similar to those of control cells. Lipid droplets in S 26948–treated cells were smaller and less abundant than those in rosiglitazone-treated cells and were indeed very similar to control cells (Fig. 2*B*).

The rate of triglyceride accumulation was the same in control and S 26948–treated cells in a time-course analysis (Fig. 2*C*). By contrast, cells treated with 100 nmol/l rosiglitazone accumulated significantly more triglycerides than control or S 26948 cells as soon as 4 days after confluence. On the other hand, S 26948 slightly induced mRNA expression of adipocyte marker genes aP2, LPL, PEPCK, and PPARγ2 but to a lesser extent than rosiglitazone (Fig. 2*D*).

Specific coactivator recruitment by S 26948. The ligand-binding domain of PPARγ interacts with cofactors such as DRIP205, CBP, PGC-1α, GRIP1, and SRC-1 (47,48). GST pull-down experiments were first carried out to assess the affinity of PPARγ for GST fusion proteins with the indicated cofactors (Fig. 3*A* and *B*). Compared with control conditions, both S 26948 and rosiglitazone at 10 μmol/l had no significant effect on the interaction between the PPARγ-binding domain and SRC-1 (Fig. 3*A*). By contrast, whereas rosiglitazone stimulated the formation of PPARγ/DRIP205 and PPARγ/PGC-1α complexes, S 26948 was unable to elicit the formation of such complexes. However, S 26948 and rosiglitazone recruited GRIP1 with a seemingly equal efficiency (Fig. 3*A* and *B*). Similar results were obtained with 1 μmol/l of each ligand (data not shown).

A mating yeast two-hybrid assay was then used to assess the affinity of these coregulators for PPARγ. End point results obtained at the highest concentrations used (50 μmol/l in this assay) fully support our results shown in panel *A* and *B* (data not shown). Results were thus expressed as the area under the curve, obtained from mating interaction assays carried out at ligand concentrations ranging from 50 nmol/l to 50 μmol/l (Fig. 3*C*). There is therefore a reflection of the affinity of PPARγ for the various coregulators used here. These affinity assays revealed again that S 26948 promotes a weaker interaction of PPARγ with DRIP205, PGCα, and SRC1—the latter being undetectable in GST pull-down assays. A similar behavior was detected for CBP, whose interaction with PPARγ was barely above threshold in GST pull-down assays. In this assay, rosiglitazone was also more efficient at displacing SMRT than S 26948. Finally, GRIP1/TIF2 exhibited an equal affinity for rosiglitazone- or S 26948–bound PPARγ. Taken collectively, these two approaches clearly suggested that S 26948 promoted a PPARγ conformation distinct from that elicited by rosiglitazone.

S 26948 is a potent antidiabetes drug. To test the possible antidiabetes effects of S 26948, 8- to 12-week-old male *ob/ob* mice were treated with 30 mg/kg S 26948, 10 mg/kg rosiglitazone, or vehicle (control mice) by daily intraperitoneal administration for 13 days. These doses were chosen based on their efficiency in reducing blood glucose levels to the same levels in preliminary pharmacokinetic studies (data not shown). As shown in Table 1, treatment with S 26948 resulted in decreased blood glucose levels (52%) and a concomitant strong reduction of plasma insulin levels (95%). This suggests that S 26948 increased insulin sensitivity. Furthermore, S 26948 treatment was capable of normalizing serum triglyceride levels (46% reduction) and lowering serum NEFA levels (55%). All these effects paralleled those of rosiglitazone treatment (Table 1).

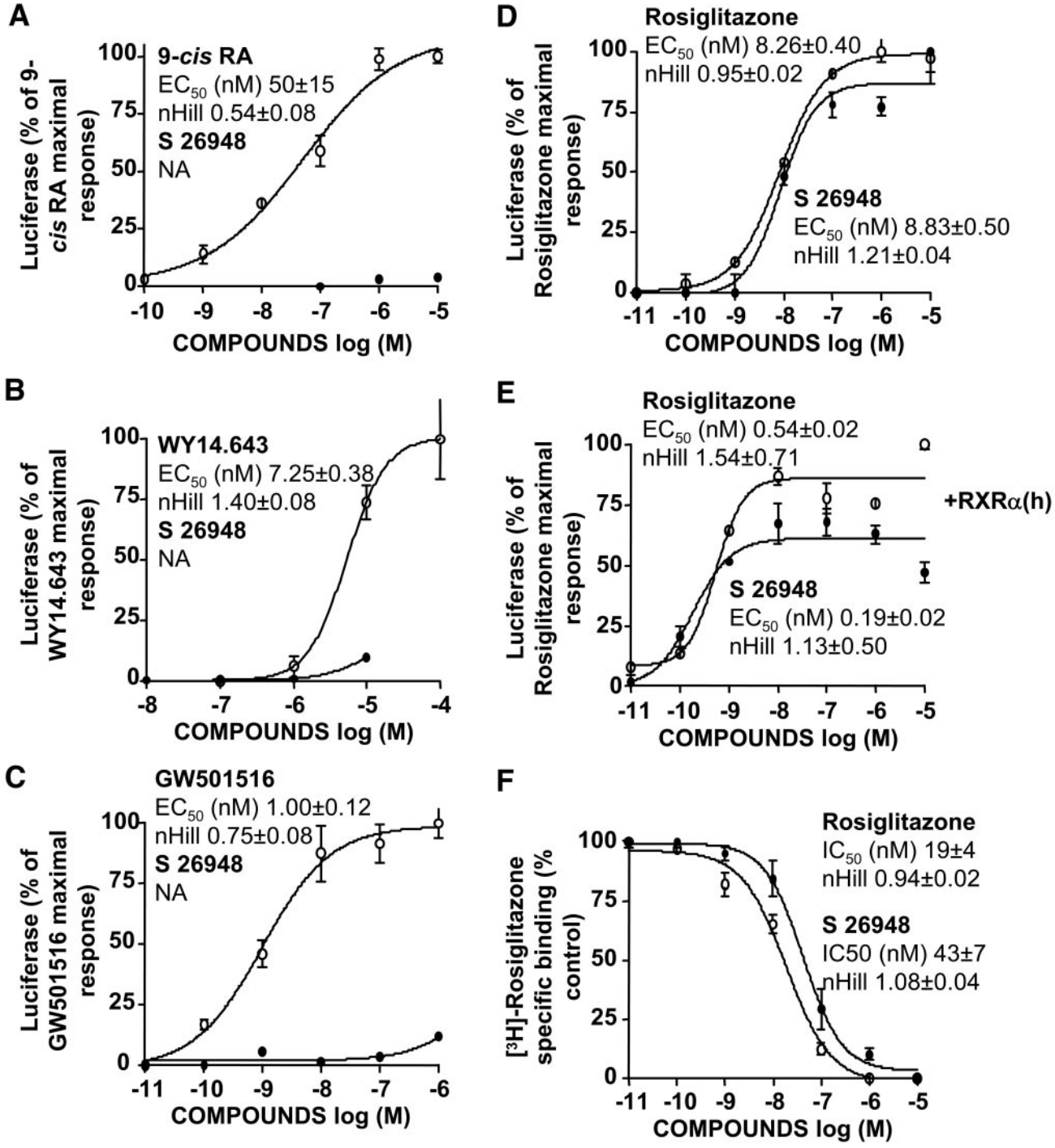

FIG. 1. In vitro profile of S 26948 and rosiglitazone. *A–D*: No activation of human RXRα, human PPARα, or human PPARβ/δ was found with S 26948. S 26948 (●) and rosiglitazone (○) activate human PPARγ in a transient transfection reporter assay. 9-*cis* retinoic acid (*A*), Wy 14,643 (*B*), GW 501516 (*C*), and rosiglitazone (*D*) (○) are used as positive control of transactivation assay for RXRα, PPARα, PPARδ, and PPARγ, respectively. COS-7 cells were transiently transfected with the luciferase reporter plasmid (pG5-TK-pGL3) in the presence of pGal4hRXR (*A*), pGal4hPPARα (*B*), pGal4hPPARβ/δ (*C*), or pGal4hPPARγ (*D*) (these vectors express chimeric proteins containing the Gal4 DNA-binding domain fused to the indicated human PPAR or RXRα ligand-binding domain coding sequence) expression vector. Cells were incubated 24 h in the presence of the indicated concentrations of S 26948 or positive control. Luciferase activity was measured and normalized to internal control β-galactosidase activity. EC_{50} is the concentration of tested compound required to induce 50% of maximal activity. Data are means ± SEM of triplicate points. *E*: COS-7 cells were transiently transfected with the full-length PPARγ (pSG5hPPARγ), RXRα (pSG5hRXRα), and reporter vector containing the hapoA-II DR-1PPRE (J6TkpGL3). Cells were incubated 24 h in the presence of the indicated concentrations of S 26948 (●) or rosiglitazone (○). Luciferase activity was measured and normalized to internal control β-galactosidase activity. EC_{50} is the concentration of tested compound required to induce 50% of maximal activity. Data are means ± SEM of triplicate points. *F*: S 26948 (●) binds PPARγ with the same affinity as rosiglitazone (○). Competition binding assays were performed using bacterial extracts containing GST-PPARγ LBD (25 μg/ml) and 4 nmol/l [^{3}H]rosiglitazone in the presence of increasing concentrations of cold S 26948 or rosiglitazone. Nonspecific binding was defined in the presence of 1 μmol/l of rosiglitazone. The K_i value is calculated according to the equation $K_i = IC_{50}/1\{+([L]/K_d)\}$, where IC_{50} is the concentration of test compound required to inhibit 50% of the specific binding of the radioligand, [L] is the concentration of the radioligand used, and K_d is the dissociation constant for the radioligand at the receptor. Data are means ± SEM of triplicate points.

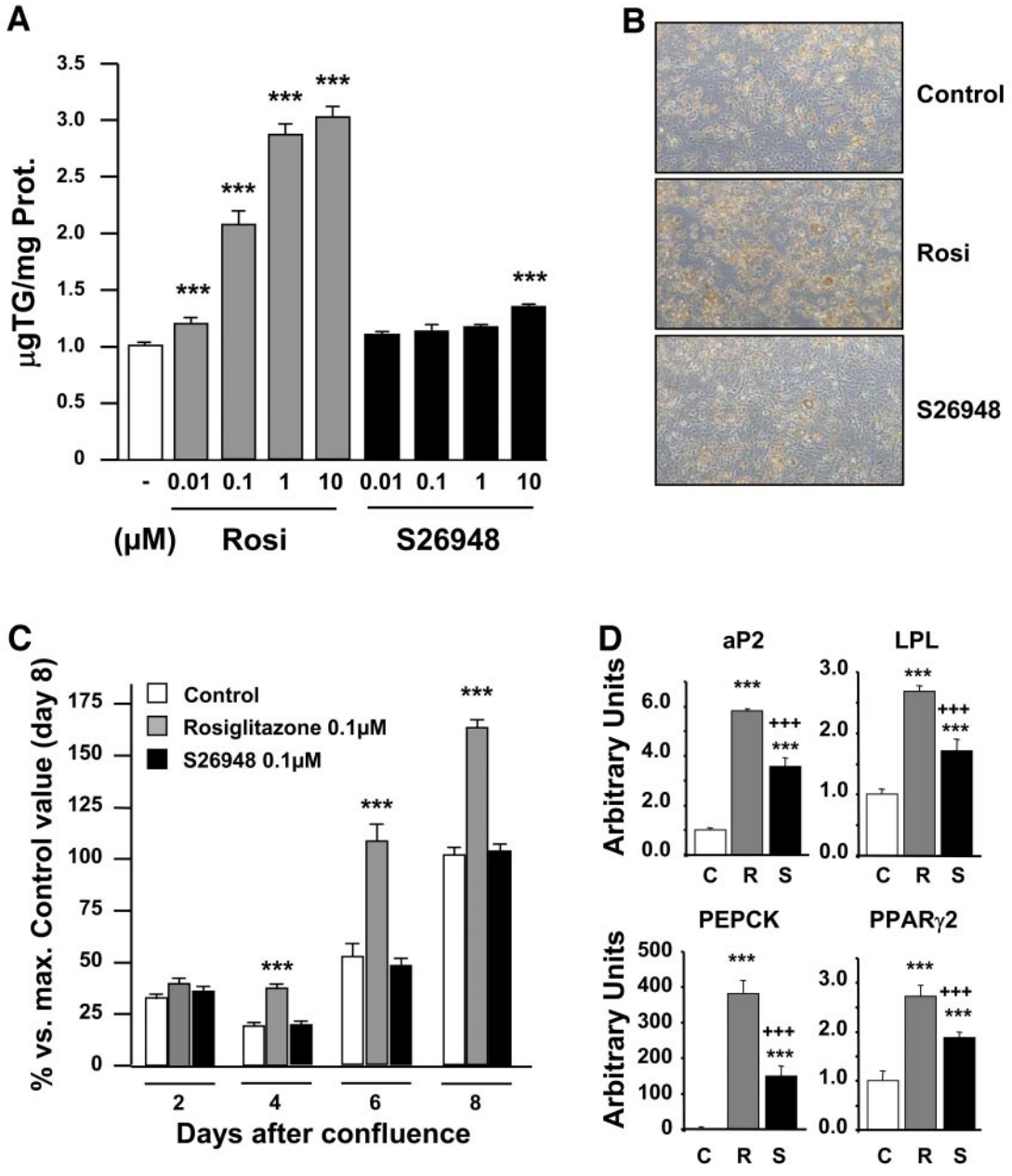

FIG. 2. Effects of S 26948 on 3T3-F442A differentiation. *A*: Dose-dependent triglyceride accumulation. *B*: Oil-red O staining. *C*: Time course of triglyceride accumulation. Data are presented as percentage vs. the maximal triglyceride accumulation of untreated (Control) cells (day 8). Data are the means ± SEM of triplicate points. *D*: mRNA expression of adipogenic genes in 3T3-F442A cells treated with vehicle, 100 nmol/l rosiglitazone, or 100 nmol/l S 26948. Total RNA was extracted from cells and subjected to real-time PCR. Cyclophilin was used as a control mRNA. Data are means ± SEM; $n = 5–6$. C, control cells; R and Rosi, rosiglitazone-treated cells; S, S 26948–treated cells; TG, triglycerides; Prot, protein. ***Significantly different from control cells $P < 0.001$; +++Significantly different from rosiglitazone–treated cells $P < 0.001$. (Please see http://dx.doi.org/10.2337/db06-1734 for a high-quality digital representation of this figure.)

S 26948 treatment does not promote body-weight gain in diabetic *ob/ob* mice. One of the undesirable effects of TZD treatment in type 2 diabetic subjects is body-weight gain (31,33,34). To determine the effects of S 26948 treatment, body weight was measured daily and body-weight gain calculated as the difference in body weight between each day and day 0. Figure 4*A* shows the body-weight gain at the end of the treatment, as well as food intake and efficiency. Whereas rosiglitazone significantly increased body weight compared with weight of controls, S 26948 had an opposite effect. Thus, at the end of the treatment, the body-weight gain was 5.52 ± 0.42 g, 3.63 ± 0.31 g, and 0.87 ± 0.82 g for rosiglitazone-, control, and S 26948–treated mice, respectively. Indeed, no difference in food intake was measured, resulting in a profoundly decreased food efficiency in the S 26948–treated mice compared either with control or rosiglitazone-treated animals.

S 26948 treatment effects on white adipose tissue weight in diabetic *ob/ob* mice. S 26948 treatment did not increase white adipose tissue (WAT) weight compared either with rosiglitazone or control mice. As expected, rosiglitazone treatment increased epidydimal (15.5 and 21.9% vs. control and S 26948–treated animals, respectively), inguinal (20 and 40.2%, respectively), and total WAT weight (as the sum of iWAT and epididimal WAT weight depots; 17.5 and 36.6%, respectively) (Fig. 4*B*). Furthermore, S 26948 treatment decreases mRNA expres-

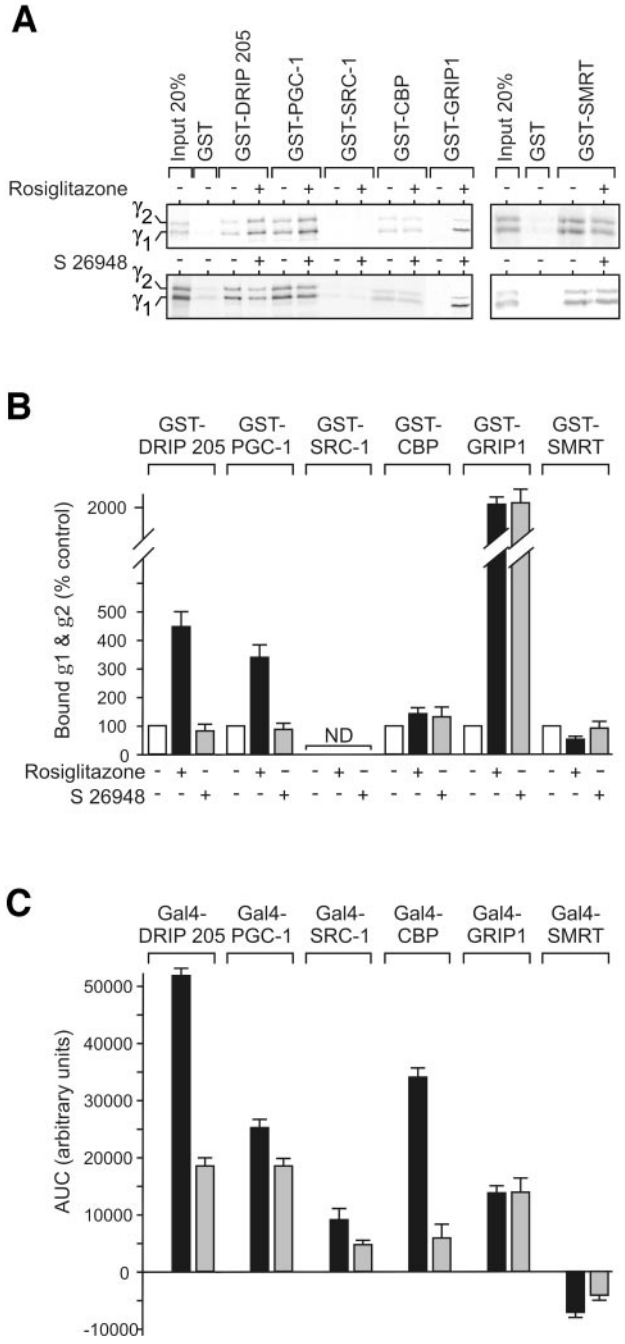

FIG. 3. In vitro profile of coactivator recruitment by S 26948 and rosiglitazone. *A*: Interaction of PPARγ with nuclear coactivators. ^{35}S-labeled PPARγ_1 and -$_2$ synthesized by in vitro coupled transcription/translation was incubated in the presence of GST or GST-DRIP205 (527–774), GST-SRC1 (382–842), GST-PGC1α (1–200), GST-CBP (1–1099), and GST-GRIP1 (563–1121). When indicated, ligands were added at 10 μmol/l final concentration for 2 h. Complexes were precipitated with Sepharose-glutathion beads, resolved by 8% SDS-PAGE, and visualized by autoradiography. *B*: Quantification of protein-protein interactions. Results shown in *A* are from three other independent experiments, quantified and expressed as a percentage of PPARγ_1 and -$_2$ bound to the fusion protein in the absence of ligand (the vehicle was DMSO 0.5%). *C*: Yeast mating interaction assays. Interaction assays were carried out at 10 different ligand concentrations, and the interaction was assayed using an α-galactosidase fluorogenic assay. Fluorescence units were plotted as a function of the ligand concentration, and the area under the curve (AUC) was calculated. A negative value indicates a decreased interaction below the "no ligand" value. The cofactor fragments used in this assay were DRIP205: amino acid 459–803, PGC1: 190–403, SRC1: 459–888, CBP: 8–93, GRIP1: 548–878, and SMRT: 373-1191.

sion of the adipogenic transcription factors PPARγ and CCAAT/enhancer-binding protein α and the adipocyte marker gene LPL in iWAT (Fig. 4*C*). The expression of the adipokines adiponectin and TNFα was also different in iWAT of S 26948–treated mice (Fig. 4*C*). Thus, whereas rosiglitazone induced increase in both adiponectin and TNFα mRNA expression, S 26948 augmented the expression of adiponectin mRNA but not that of TNFα. Histological examination of the tissue also revealed changes in the morphology of the cells (Fig. 5*A*). Thus, both rosiglitazone- and S 26948–treated mice presented an increased number of small adipocytes in WAT deposits, most of them being positive for UCP1 (Fig. 5*A*). Nevertheless, only adipocytes from S 26948–treated animals were smaller when measured as adipocyte area (Fig. 5*B*) or as adipocyte size distribution (Fig. 5*C*). Interscapular brown adipose tissue weight was significantly increased in rosiglitazone-treated animals (110% increase vs. control mice and 45% vs. S 26948–treated animals) (Fig. 4*B*), with bigger cells and increased lipid droplets compared with control or S 26948–treated mice (Fig. 5*D*).

S 26948 increases hepatic lipid oxidation. Knowing the lipid profile, body and adipose tissue weight profiles, and adipocyte characteristics of the S 26948–treated mice, we sought to know whether this compound could exert its effects in other tissue. Skeletal muscle (gastrocnemius muscle) weight was similarly reduced in rosiglitazone- and S 26948–treated mice, but liver weight was specifically decreased in S 26948–treated animals (Fig. 6*A*) compared with both untreated and rosiglitazone-treated animals. Histological examination of the livers revealed that S 26948 was able to notably reduce lipid droplets in hepatocytes (Fig. 6*C*) by increasing the lipid oxidation capacity of the tissue (Fig. 6*C* and *D*).

S 26948 improves lipid parameters and reduces atherosclerotic lesions in E2-KI mice. To investigate the effects of S 26948 on dyslipidemia and atherosclerosis, homozygous human apoE2 knockin (E2-KI) mice were used. These mice display mixed dyslipidemia and develop atherosclerotic plaques (43). Male E2-KI mice were fed a Western diet and treated with or without rosiglitazone or S 26948 for 9 weeks. Compared with those in control mice, S 26948 reduces plasma total cholesterol ($P < 0.001$) and triglyceride ($P < 0.05$) concentrations with a decrease of non-HDL cholesterol ($P < 0.001$) levels (Table 2). Rosiglitazone had a tendency to reduce (NS) total cholesterol and non-HDL cholesterol (NS) levels (Table 2). Triglyceride levels did not change in the rosiglitazone-treated mice. HDL cholesterol levels were similar between the groups. Analysis of cholesterol and triglyceride distribution profiles confirmed the lipid results: S 26948 reduced cholesterol and triglyceride contents in the LDLs (including VLDL, intermediate-density lipoprotein [IDL], and LDL) (Fig. 6*A* and *B*). Rosiglitazone only slightly reduced cholesterol in the IDL+LDL fractions (Fig. 7*A* and *B*).

The effects on atherosclerosis were assessed in these mice at the end of treatment by measuring Oil red O–stained surfaces at the aortic sinus. S 26948 significantly reduced atherosclerotic lesion surfaces by 46% compared with those in control mice (0.033 ± 0.014 vs. 0.061 ± 0.015 mm^2, $P < 0.01$) (Fig. 8*A* and *B*). In contrast, rosiglitazone had no effect on atherosclerotic lesion size (0.062 ± 0.022 mm^2) (Fig. 8*A* and *B*).

TABLE 1
S 26948 effects on glucose, triglyceride, NEFA, and insulin serum levels in *ob/ob* mice

Ob/ob mice	Glucose (mmol/l)	Triglycerides (g/l)	NEFA (mmol/l)	Insulin (ng/ml)
Control	13.5 ± 1.5	1.43 ± 0.19	2.81 ± 0.46	63.4 ± 3.6
Rosiglitazone (10 mg · kg^{-1} · day^{-1})	7.3 ± 0.3*	0.82 ± 0.06†	1.15 ± 0.17†	2.3 ± 0.5*
S 26948 (30 mg · kg^{-1} · day^{-1})	7.5 ± 0.6*	0.69 ± 0.10†	0.98 ± 0.25†	3.1 ± 0.4*

Data are means ± SEM (n = 5–7). One-way ANOVA denoted significant differences between groups for glucose (P = 0.0005), triglyceride (P = 0.0043), NEFA (P = 0.0028), and insulin (P = 0.0010). *Significantly different from control mice, $P < 0.001$; †significantly different from control mice, $P < 0.01$.

DISCUSSION

The results of the current study establish that S 26948, a non-TZD compound, is a new SPPARM that, by contrast to most of the molecules developed so far, does not promote adipogenesis in vitro and in vivo. Furthermore, S 26948 has in vivo antidiabetes and antiatherogenic activity, improves insulin action, and corrects dyslipidemia in rodent models.

Reporter gene assays established that S 26948 is a full PPARγ-specific agonist, at least as potent as rosiglitazone, having similar EC_{50} at the nanomole per liter order (Fig. 1*D*) and an affinity of S 26948 for its receptor as high as that of rosiglitazone (Fig. 1*F*). However, the finding that it has no effect on adipogenesis—in addition to the significant effect in reducing atherosclerosis—showed functional differences with rosiglitazone and other PPARγ agonists (21–27). This establishes S 26948 as a new specific PPARγ modulator that is able to drive normal adipocyte differentiation—in contrast to rosiglitazone, which exacerbates this process. Thus, 3T3-F442A cells differentiated with rosiglitazone largely increased triglyceride content and PPARγ adipocyte target gene expression such as LPL and aP2, whereas S 26948 did not influence these parameters (Fig. 2) in sharp contrast with other PPARγ ligands (22,23).

The mechanisms by which nuclear receptors regulate transcription of target genes are not fully understood. However, evidence indicates that ligand binding results in a conformational change that allows the dissociation of corepressors (such as NcoR) and SMRT, as well as the association of coactivators (such as SRC1, DRIP205, CBP/p300, or PGC1α, among others) (48). Interestingly, it is clear from our data that rosiglitazone and S 26948 did not induce a similar pattern of cofactor recruitment by PPARγ (Fig. 2). Whereas rosiglitazone induced the recruitment of DRIP205 and PGC1α, S 26948 was unable to trigger these interactions, providing evidence of structural differences between rosiglitazone and S 26948 liganded PPARγ, which may explain in part the different biological properties of these drugs in vitro and in vivo (see below). Since DRIP205 (TRAP220) has been described as a coactivator of PPARγ required for adipogenesis (49), the decreased adipogenic activity of S 26948 might be explained in part by the lower

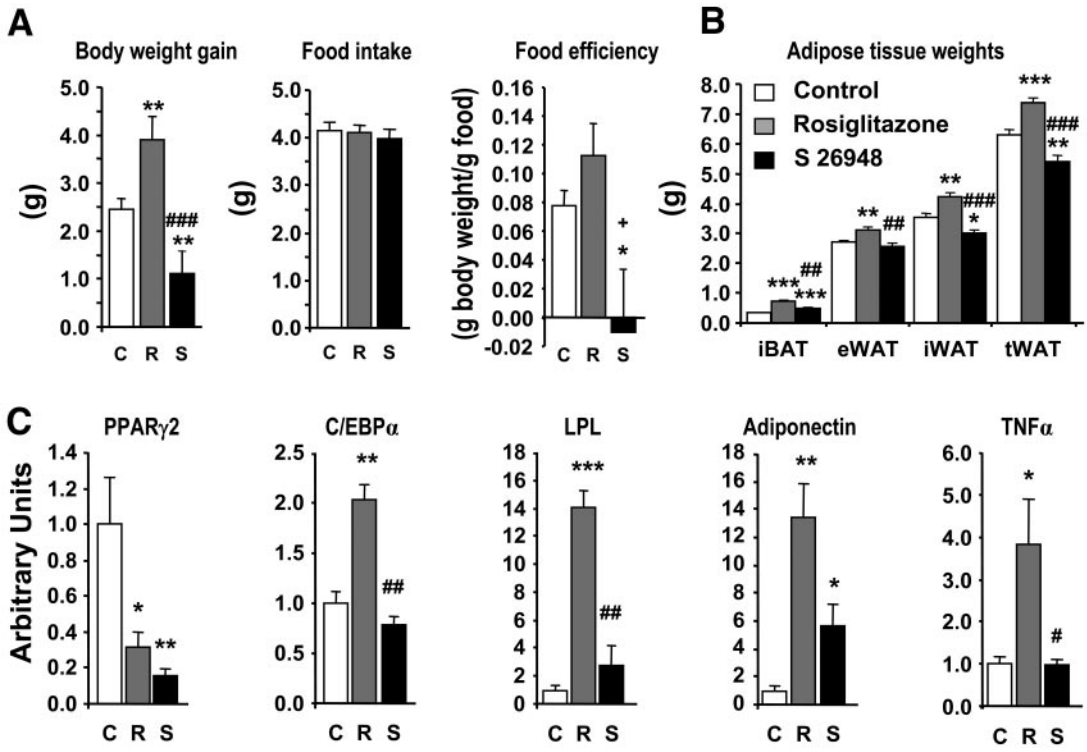

FIG. 4. In vivo properties of S 26948 compared with rosiglitazone. Body weight gain, daily food intake, and efficiency (*A*) and adipose tissue weights (*B*) of *ob/ob* mice after 13 days of treatment with S 26948 or rosiglitazone. iBAT, interescapular brown adipose tissue; eWAT, epididimal WAT; tWAT, total WAT calculated as the sum of iWAT and eWAT. Data are means ± SEM; n = 12–24. *C*: mRNA expression of adipogenic genes in iWAT of treated animals. Total RNA was extracted from iWAT and subjected to real-time PCR. Cyclophilin was used as a control mRNA. Data are means ± SEM; n = 5–8. C/EBPα, CCAAT/enhancer-binding protein α.

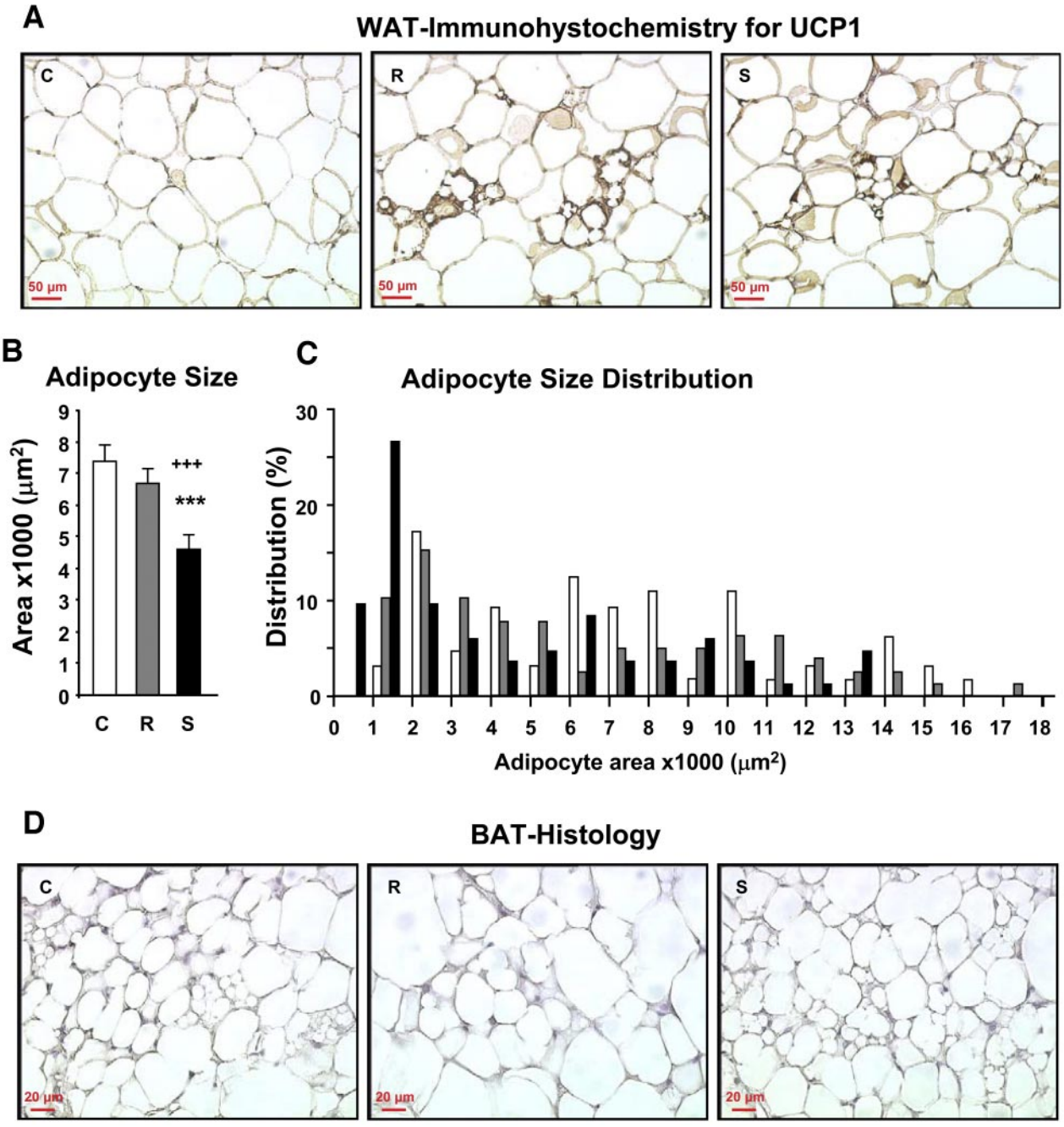

FIG. 5. *A*: **Immunohistochemistry of UCP1. iWAT from treated mice was fixed and subjected to UCP1 detection. Small brown-colored cells are positive cells for UCP1. Adipocyte area (*B*) and distribution (*C*) of treated animals. *D*: Histological sections of interescapular brown adipose tissue (iBAT) from treated mice. *Significantly different from control mice, $P < 0.05$; **$P < 0.01$; ***$P < 0.001$. #Significantly different from rosiglitazone-treated mice, $P < 0.05$; ##$P < 0.01$; ###$P < 0.01$. (Please see http://dx.doi.org/10.2337/db06-1734 for a high-quality digital representation of this figure.)**

efficiency of S 26948 than rosiglitazone to recruit this coactivator.

Recently it has been proposed that moderate activation of PPARγ would improve metabolic features without increasing adipocyte differentiation (50). Moderated activation of PPARγ could be achieved by two mechanisms: *1*) by partial agonism or antagonism of the receptor or *2*) by differential coactivator recruitment. S 26948 exerts its activity as a full agonist of PPARγ, as demonstrated by the binding experiences, but with a specific coactivator recruitment that decreases its adipogenic capacity compared with rosiglitazone and thus acts as a specific modulator of PPARγ activity.

These in vitro results are consistent with the in vivo data on body weight in obese mice. It is well known that most PPARγ ligands are able to normalize glycemia and insulinemia in spite of increasing body weight (22,24). This has first been observed with TZDs in animal studies (31,32,51) and then confirmed in mildly obese humans treated with such compounds (33,34). In humans, the severity of weight gain is proportional to the level of glycemic control achieved and is thus often related to the dose used. In the present study, we show that rosiglitazone, a full PPARγ agonist, has a net effect on body-weight gain. Indeed, a clear increase in adipose tissue mass was observed upon rosiglitazone treatment, whereas S 26948

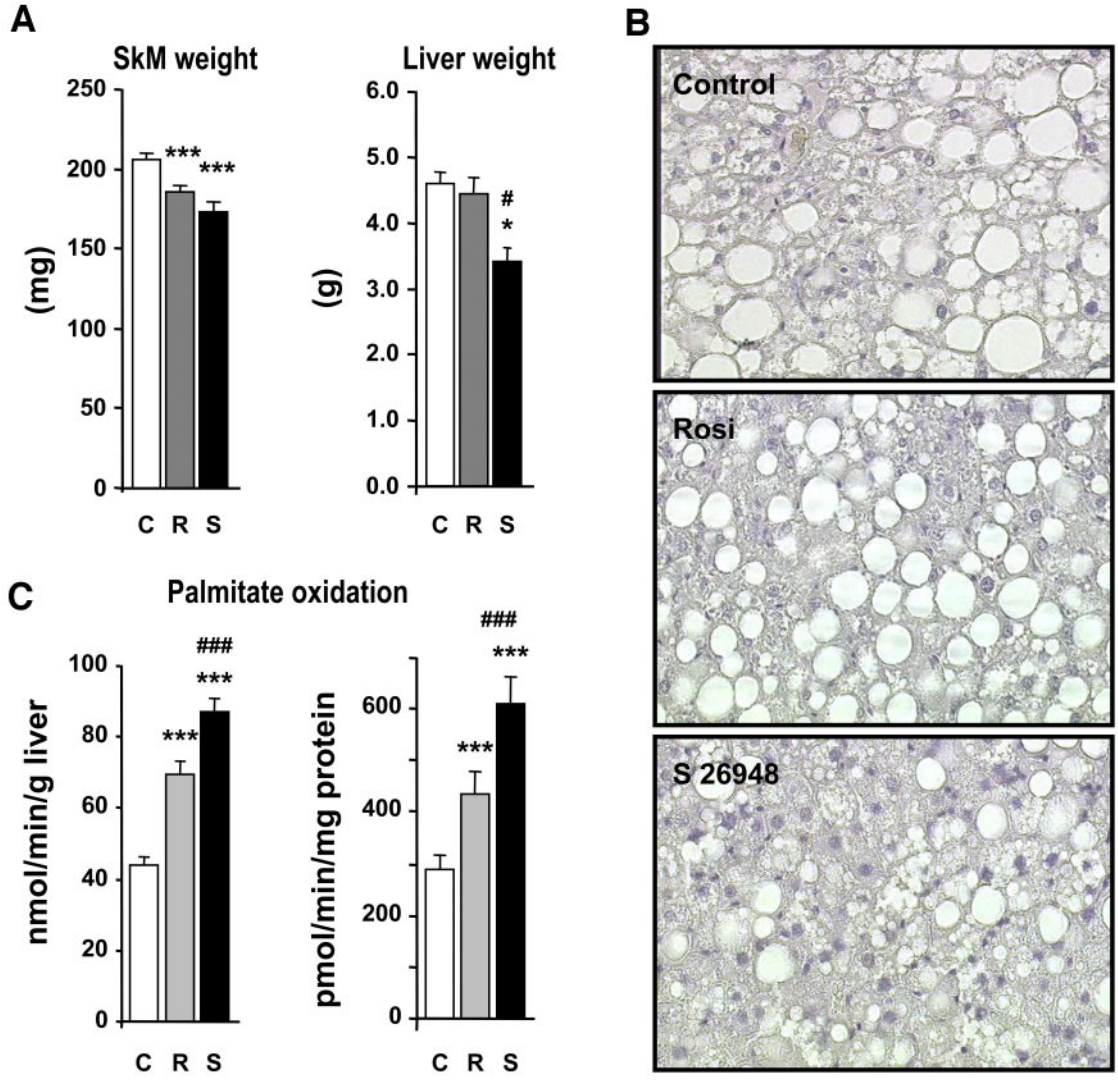

FIG. 6. S 26948 treatement increases hepatic lipid oxidation. *A*: Skeletal muscle and liver weights of *ob/ob* treated mice. *B*: Histological examination of livers from treated animals. *C* and *D*: Palmitate oxidation was assessed in liver homogenates of *ob/ob* treated mice and corrected either by gram of liver (*C*) or by milligram of protein (*D*). *Significantly different from control mice, $P < 0.05$; ***$P < 0.001$. #Significantly different from rosiglitazone-treated mice, $P < 0.05$; ###$P < 0.01$. (Please see http://dx.doi.org/10.2337/db06-1734 for a high-quality digital representation of this figure.)

had an opposite effect. This is in accordance with the in vitro results.

Compared with rosiglitazone, S 26948 was as potent to lower glucose, NEFA, triglyceride, and insulin levels in *ob/ob* mice—a model of type 2 diabetes (Table 1). The exact mechanism by which PPARγ agonists exert their insulin-sensitizing effect is still not well understood. This could be related to the ability to decrease serum free fatty acids (FFAs), since increased FFA levels have been shown to induce insulin resistance (52). Lowered FFA level, observed on TZD treatment, has been proposed to be the consequence (in adipose tissue) of both an increased storage and/or a decreased release. These explanations might hold true for rosiglitazone but cannot occur with regard to S 26948, which did not promote body-weight gain. An alternative explanation for the beneficial effect of S 26948 on glucose homeostasis might be its distinctive regulatory properties in other organ(s), such as liver. In

TABLE 2
S 26948 effects on lipid parameters in E2-KI mice fed a Western diet

E2-KI mice	Total cholesterol (mg/dl)	HDL cholesterol (mg/dl)	Non-HDL cholesterol (mg/dl)	Triglycerides (mg/dl)
Control	936 ± 81	60 ± 9	876 ± 75	331 ± 78
Rosiglitazone (10 mg · kg^{-1} · day^{-1})	730 ± 62	68 ± 13	662 ± 70	348 ± 45
S 26948 (30 mg · kg^{-1} · day^{-1})	500 ± 67*	72 ± 13	428 ± 69*	154 ± 16†

Data are means ± SEM. One-way ANOVA denoted significant differences between groups for total cholesterol ($P = 0.001$), non-HDL cholesterol ($P = 0.001$), and triglycerides ($P = 0.022$). *Significantly different from control mice, $P < 0.001$; †significantly different from control mice, $P < 0.05$.

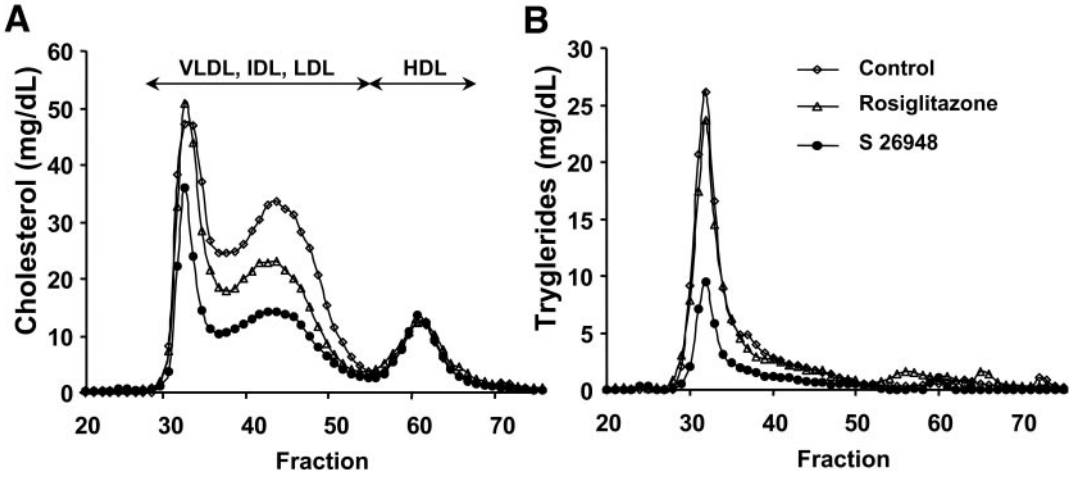

FIG. 7. Cholesterol and triglyceride distribution into the lipoproteins. Cholesterol (*A*) and triglycerides (*B*) were measured in lipoproteins separated by gel filtration chromatography from pooled plasma of E2-KI mice fed a Western diet (Control; □) supplemented with rosiglitazone (△) or S 26948 (●) for 9 weeks.

fact, both molecules increased lipid oxidation in liver, but S 26948 appears to have a greater effect than rosiglitazone (higher palmitic oxidation and lower lipid infiltration) (Fig. 6). This amelioration on hepatic lipid catabolism may explain part of the glucose homeostasis improvement and lipid-lowering effect of S 26948. In addition to this increment of hepatic lipid oxidation, also noted is the enhanced expression of UCP1 in adipose tissue of treated animals (Fig. 5*A*), which may also be involved in increasing energy expenditure in this tissue, although no obvious differences could be observed between rosiglitazone and S 26948. Selective biological effect(s) of S 26948, when compared with other PPARγ agonists, might stem from its inability to promote the recruitment of two coactivators, DRIP205 and PGC-1, to PPARγ in our conditions. As both have been shown to have a crucial role in adipocyte differentiation, this may provide a molecular explanation for the nonadipogenic properties of S 26948. By extension, the effect of S 26948 on glucose homeostasis may be related to its specific properties on coactivator recruitment, consistent with the concept of SPPARM (12,13). In this regard, the differential regulation of adiponectin and TNFα of both compounds (Fig. 4*C*) may also be the result of their special coactivator recruitment and indeed contribute to the glucose- and lipid-lowering effects of S 26948. Thus, S 26948 restores the balance between adipose adiponectin and TNFα gene expression in our in vivo model, which is in clear contrast to rosiglitazone.

Different studies have documented that PPAR ligands inhibit the development of atherosclerosis in different mouse models (56). In E2-KI mice, PPARγ agonists like rosiglitazone or pioglitazone do not reduce the development of atherosclerosis (57). In the present study, we confirmed that in this model rosiglitazone has no significant effect on plasma lipoprotein (Table 2 and Fig. 6) or atherosclerosis (Fig. 7). By contrast, S 26948 reduced atherosclerosis. This effect was associated with a decrease of cholesterol and triglyceride content in the LDL particles (VLDL, IDL, and LDL). This suggests that the reduction of

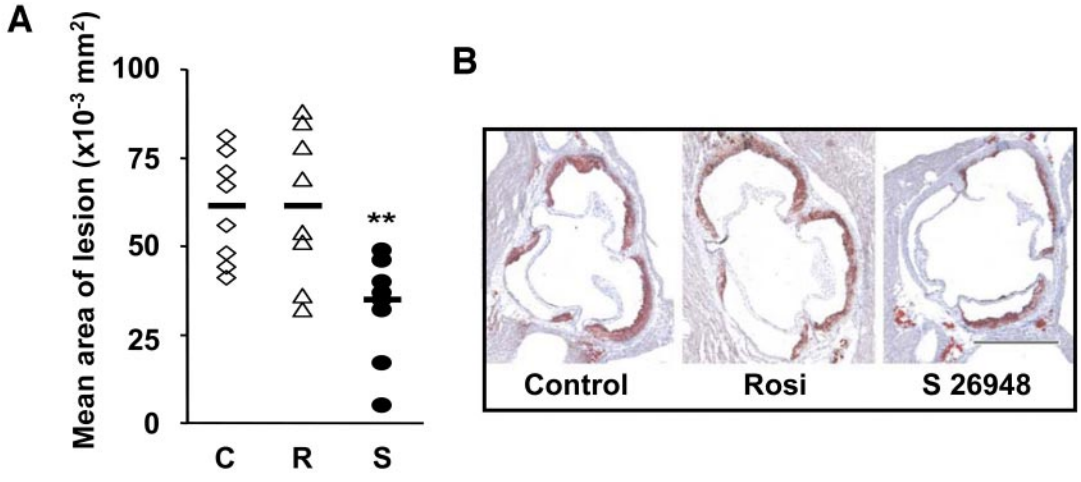

FIG. 8. Atherosclerotic lesions surface area in the aortic sinus of E2-KI mice. *A*: Oil red O staining of atherosclerotic lesions in serial sections between the valves and the aortic crosses was measured. The graph shows atherosclerotic lesion surface area quantification. Each symbol represents the average area staining in 10 aortic sections from individual animals, and horizontal bars represent median of the mean lesion area. E2-KI mice fed a Western diet (n = 8) (C) (□), supplemented with rosiglitazone (n = 8) (R) (△) or S 26948 (n = 8) (S) (●). Statistically significant differences between groups are indicated by asterisks (Mann-Whitney U test, $^{**}P < 0.01$). *B*: Representative photomicrographs showing atherosclerotic lesions in the aortic sinus of control or treated mice. Bar = 0.5 mm. (Please see http://dx.doi.org/10.2337/db06-1734 for a high-quality digital representation of this figure.)

atherosclerosis with S 26948 treatment is in part due to a decrease of atherogenic lipoproteins.

In summary, we identified a new compound (S 26948) that exerts antidiabetes effects similar to most of the other PPARγ ligands. However, when compared with these ligands, S 26948 is highly specific and selective for PPARγ and does not promote adipogenesis and body-weight gain. Furthermore, it shows a strong efficiency in correcting dyslipidemia and atherosclerosis. Although the exact mechanism beyond these effects remains to be determined, S 26948 or related compounds might represent a new class of therapeutic molecules for the treatment of type 2 diabetes and atherosclerosis.

ACKNOWLEDGMENTS

We thank B. Spiegelman (Dana-Farber Institute, Boston, MA), B.W. O'Malley (Baylor College of Medecine, Houston, TX), C. Rachez (INSERM U459, Lille, France), and L.P. Freedman (Merck, West Point, PA) for the gift of plasmids.

We fully acknowledge M. Coevoet, J. Vanhoutte, M. Nibbelink, Y. Jeanson, and M. Boisson for excellent technical assistance, as well as the assistance of the staff of the animal quarter of the IFR31, in particular Y. Barreira and J.M. Lerme.

REFERENCES

1. Giguere V: Orphan nuclear receptors: from gene to function. *Endocr Rev* 20:689–725, 1999
2. Tontonoz P, Hu E, Graves RA, Budavari AI, Spiegelman BM: mPPAR gamma 2: tissue-specific regulator of an adipocyte enhancer. *Genes Dev* 8:1224–1234, 1994
3. Tontonoz P, Hu E, Spiegelman BM: Stimulation of adipogenesis in fibroblasts by PPAR gamma 2, a lipid-activated transcription factor. *Cell* 79:1147–1156, 1994
4. Vidal-Puig AJ, Considine RV, Jimenez-Linan M, Werman A, Pories WJ, Caro JF, Flier JS: Peroxisome proliferator-activated receptor gene expression in human tissues: effects of obesity, weight loss, and regulation by insulin and glucocorticoids. *J Clin Invest* 99:2416–2422, 1997
5. Ricote M, Li AC, Willson TM, Kelly CJ, Glass CK: The peroxisome proliferator-activated receptor-gamma is a negative regulator of macrophage activation. *Nature* 391:79–82, 1998
6. Kubota N, Terauchi Y, Miki H, Tamemoto H, Yamauchi T, Komeda K, Satoh S, Nakano R, Ishii C, Sugiyama T, Eto K, Tsubamoto Y, Okuno A, Murakami K, Sekihara H, Hasegawa G, Naito M, Toyoshima Y, Tanaka S, Shiota K, Kitamura T, Fujita T, Ezaki O, Aizawa S, Kadowaki T, et al.: PPAR gamma mediates high-fat diet-induced adipocyte hypertrophy and insulin resistance. *Mol Cell* 4:597–609, 1999
7. Rosen ED, Sarraf P, Troy AE, Bradwin G, Moore K, Milstone DS, Spiegelman BM, Mortensen RM: PPAR gamma is required for the differentiation of adipose tissue in vivo and in vitro. *Mol Cell* 4:611–617, 1999
8. Hu E, Tontonoz P, Spiegelman BM: Transdifferentiation of myoblasts by the adipogenic transcription factors PPAR gamma and C/EBP alpha. *Proc Natl Acad Sci U S A* 92:9856–9860, 1995
9. Chawla A, Boisvert WA, Lee CH, Laffitte BA, Barak Y, Joseph SB, Liao D, Nagy L, Edwards PA, Curtiss LK, Evans RM, Tontonoz P: A PPAR gamma-LXR-ABCA1 pathway in macrophages is involved in cholesterol efflux and atherogenesis. *Mol Cell* 7:161–171, 2001
10. Chinetti G, Lestavel S, Bocher V, Remaley AT, Neve B, Torra IP, Teissier E, Minnich A, Jaye M, Duverger N, Brewer HB, Fruchart JC, Clavey V, Staels B: PPAR-alpha and PPAR-gamma activators induce cholesterol removal from human macrophage foam cells through stimulation of the ABCA1 pathway. *Nat Med* 7:53–58, 2001
11. Li AC, Brown KK, Silvestre MJ, Willson TM, Palinski W, Glass CK: Peroxisome proliferator-activated receptor gamma ligands inhibit development of atherosclerosis in LDL receptor-deficient mice. *J Clin Invest* 106:523–531, 2000
12. Olefsky JM: Treatment of insulin resistance with peroxisome proliferator-activated receptor gamma agonists. *J Clin Invest* 106:467–472, 2000
13. Sporn MB, Suh N, Mangelsdorf DJ: Prospects for prevention and treatment of cancer with selective PPARgamma modulators (SPARMs). *Trends Mol Med* 7:395–400, 2001
14. Kliewer SA, Lenhard JM, Willson TM, Patel I, Morris DC, Lehmann JM: A prostaglandin J2 metabolite binds peroxisome proliferator-activated receptor gamma and promotes adipocyte differentiation. *Cell* 83:813–819, 1995
15. Forman BM, Tontonoz P, Chen J, Brun RP, Spiegelman BM, Evans RM: 15-Deoxy-delta 12, 14-prostaglandin J2 is a ligand for the adipocyte determination factor PPAR gamma. *Cell* 83:803–812, 1995
16. Kliewer SA, Sundseth SS, Jones SA, Brown PJ, Wisely GB, Koble CS, Devchand P, Wahli W, Willson TM, Lenhard JM, Lehmann JM: Fatty acids and eicosanoids regulate gene expression through direct interactions with peroxisome proliferator-activated receptors alpha and gamma. *Proc Natl Acad Sci U S A* 94:4318–4323, 1997
17. Krey G, Braissant O, L'Horset F, Kalkhoven E, Perroud M, Parker MG, Wahli W: Fatty acids, eicosanoids, and hypolipidemic agents identified as ligands of peroxisome proliferator-activated receptors by coactivator-dependent receptor ligand assay. *Mol Endocrinol* 11:779–791, 1997
18. Davies SS, Pontsler AV, Marathe GK, Harrison KA, Murphy RC, Hinshaw JC, Prestwich GD, Hilaire AS, Prescott SM, Zimmerman GA, McIntyre TM: Oxidized alkyl phospholipids are specific, high affinity peroxisome proliferator-activated receptor gamma ligands and agonists. *J Biol Chem* 276:16015–16023, 2001
19. Lehmann JM, Moore LB, Smith-Oliver TA, Wilkison WO, Willson TM, Kliewer SA: An antidiabetic thiazolidinedione is a high affinity ligand for peroxisome proliferator-activated receptor gamma (PPAR gamma). *J Biol Chem* 270:12953–12956, 1995
20. Berger J, Bailey P, Biswas C, Cullinan CA, Doebber TW, Hayes NS, Saperstein R, Smith RG, Leibowitz MD: Thiazolidinediones produce a conformational change in peroxisomal proliferator-activated receptor-gamma: binding and activation correlate with antidiabetic actions in db/db mice. *Endocrinology* 137:4189–4195, 1996
21. Fukui Y, Masui S, Osada S, Umesono K, Motojima K: A new thiazolidinedione, NC-2100, which is a weak PPAR-γ activator, exhibits potent antidiabetic effects and induces uncoupling protein 1 in white adipose tissue of KKAy obese mice. *Diabetes* 49:759–767, 2000
22. Brown KK, Henke BR, Blanchard SG, Cobb JE, Mook R, Kaldor I, Kliewer SA, Lehmann JM, Lenhard JM, Harrington WW, Novak PJ, Faison W, Binz JG, Hashim MA, Oliver WO, Brown HR, Parks DJ, Plunket KD, Tong WQ, Menius JA, Adkison K, Noble SA, Willson TM: A novel *N*-aryl tyrosine activator of peroxisome proliferator–activated receptor-γ reverses the diabetic phenotype of the Zucker diabetic fatty rat. *Diabetes* 48:1415–1424, 1999
23. Rocchi S, Picard F, Vamecq J, Gelman L, Potier N, Zeyer D, Dubuquoy L, Bac P, Champy MF, Plunket KD, Leesnitzer LM, Blanchard SG, Desreumaux P, Moras D, Renaud JP, Auwerx J: A unique PPARgamma ligand with potent insulin-sensitizing yet weak adipogenic activity. *Mol Cell* 8:737–747, 2001
24. Ostberg T, Svensson S, Selen G, Uppenberg J, Thor M, Sundbom M, Sydow-Backman M, Gustavsson AL, Jendeberg L: A new class of peroxisome proliferator-activated receptor agonists with a novel binding epitope shows antidiabetic effects. *J Biol Chem* 279:41124–41130, 2004
25. Schupp M, Clemenz M, Gineste R, Witt H, Janke J, Helleboid S, Hennuyer N, Ruiz P, Unger T, Staels B, Kintscher U: Molecular characterization of new selective peroxisome proliferator–activated receptor γ modulators with angiotensin receptor blocking activity. *Diabetes* 54:3442–3452, 2005
26. Allen T, Zhang F, Moodie SA, Clemens LE, Smith A, Gregoire F, Bell A, Muscat GE, Gustafson TA: Halofenate is a selective peroxisome proliferator–activated receptor γ modulator with antidiabetic activity. *Diabetes* 55:2523–2533, 2006
27. Kim KR, Lee JH, Kim SJ, Rhee SD, Jung WH, Yang SD, Kim SS, Ahn JH, Cheon HG: KR-62980: a novel peroxisome proliferator-activated receptor gamma agonist with weak adipogenic effects. *Biochem Pharmacol* 72:446–454, 2006
28. Goldstein BJ: Differentiating members of the thiazolidinedione class: a focus on efficacy. *Diabete Metab Res Rev* 18 (Suppl. 2):S16–S22, 2002
29. Phillips LS, Grunberger G, Miller E, Patwardhan R, Rappaport EB, Salzman A: Once- and twice-daily dosing with rosiglitazone improves glycemic control in patients with type 2 diabetes. *Diabetes Care* 24:308–315, 2001
30. Oakes ND, Camilleri S, Furler SM, Chisholm DJ, Kraegen EW: The insulin sensitizer, BRL 49653, reduces systemic fatty acid supply and utilization and tissue lipid availability in the rat. *Metabolism* 46:935–942, 1997
31. Schwartz S, Raskin P, Fonseca V, Graveline JF: Effect of troglitazone in insulin-treated patients with type II diabetes mellitus: Troglitazone and Exogenous Insulin Study Group. *N Engl J Med* 338:861–866, 1998
32. Chaput E, Saladin R, Silvestre M, Edgar AD: Fenofibrate and rosiglitazone lower serum triglycerides with opposing effects on body weight. *Biochem Biophys Res Commun* 271:445–450, 2000
33. Kelly IE, Han TS, Walsh K, Lean ME: Effects of a thiazolidinedione

compound on body fat and fat distribution of patients with type 2 diabetes. *Diabetes Care* 22:288–293, 1999
34. Miyazaki Y, Glass L, Triplitt C, Matsuda M, Cusi K, Mahankali A, Mahankali S, Mandarino LJ, DeFronzo RA: Effect of rosiglitazone on glucose and non-esterified fatty acid metabolism in type II diabetic patients. *Diabetologia* 44:2210–2219, 2001
35. Reasner CA: Where thiazolidinediones will fit. *Diabete Metab Res Rev* 18 (Suppl. 2):S30–S35, 2002
36. Etgen GJ, Oldham BA, Johnson WT, Broderick CL, Montrose CR, Brozinick JT, Misener EA, Bean JS, Bensch WR, Brooks DA, Shuker AJ, Rito CJ, McCarthy JR, Ardecky RJ, Tyhonas JS, Dana SL, Bilakovics JM, Paterniti JR Jr, Ogilvie KM, Liu S, Kauffman RF: A tailored therapy for the metabolic syndrome: the dual peroxisome proliferator–activated receptor-α/γ agonist LY465608 ameliorates insulin resistance and diabetic hyperglycemia while improving cardiovascular risk factors in preclinical models. *Diabetes* 51:1083–1087, 2002
37. Blanc-Delmas E, Lebegue N, Wallez V, Leclerc V, Yous S, Carato P, Farce A, Bennejean C, Renard P, Caignard DH, Audinot-Bouchez V, Chomarat P, Boutin J, Hennuyer N, Louche K, Carmona MC, Staels B, Penicaud L, Casteilla L, Lonchampt M, Dacquet C, Chavatte P, Berthelot P, Lesieur D: Novel 1,3-dicarbonyl compounds having 2(3H)-benzazolonic heterocycles as PPARgamma agonists. *Bioorg Med Chem* 14:7377–7391, 2006
38. Raspe E, Madsen L, Lefebvre AM, Leitersdorf I, Gelman L, Peinado-Onsurbe J, Dallongeville J, Fruchart JC, Berge R, Staels B: Modulation of rat liver apolipoprotein gene expression and serum lipid levels by tetradecylthioacetic acid (TTA) via PPARalpha activation. *J Lipid Res* 40:2099–2110, 1999
39. Staels B, Koenig W, Habib A, Merval R, Lebret M, Torra IP, Delerive P, Fadel A, Chinetti G, Fruchart JC, Najib J, Maclouf J, Tedgui A: Activation of human aortic smooth-muscle cells is inhibited by PPARalpha but not by PPARgamma activators. *Nature* 393:790–793, 1998
40. Ferry G, Bruneau V, Beauverger P, Goussard M, Rodriguez M, Lamamy V, Dromaint S, Canet E, Galizzi JP, Boutin JA: Binding of prostaglandins to human PPARgamma: tool assessment and new natural ligands. *Eur J Pharmacol* 417:77–89, 2001
41. Lefebvre B, Mouchon A, Formstecher P, Lefebvre P: H11–H12 loop retinoic acid receptor mutants exhibit distinct trans-activating and trans-repressing activities in the presence of natural or synthetic retinoids. *Biochemistry* 37:9240–9249, 1998
42. Mouchon A, Delmotte MH, Formstecher P, Lefebvre P: Allosteric regulation of the discriminative responsiveness of retinoic acid receptor to natural and synthetic ligands by retinoid X receptor and DNA. *Mol Cell Biol* 19:3073–3085, 1999
43. Sullivan PM, Mezdour H, Quarfordt SH, Maeda N: Type III hyperlipoproteinemia and spontaneous atherosclerosis in mice resulting from gene replacement of mouse Apoe with human Apoe*2. *J Clin Invest* 102:130–135, 1998
44. Baddeley AJ, Gundersen HJ, Cruz-Orive LM: Estimation of surface area from vertical sections. *J Microsc* 142:259–276, 1986
45. Carmona MC, Iglesias R, Obregon MJ, Darlington GJ, Villarroya F, Giralt M: Mitochondrial biogenesis and thyroid status maturation in brown fat require CCAAT/enhancer-binding protein alpha. *J Biol Chem* 277:21489–21498, 2002
46. Carmona MC, Louche K, Nibbelink M, Prunet B, Bross A, Desbazeille M, Dacquet C, Renard P, Casteilla L, Penicaud L: Fenofibrate prevents rosiglitazone-induced body weight gain in ob/ob mice. *Int J Obes (Lond)* 29:864–871, 2005
47. Furnsinn C, Waldhausl W: Thiazolidinediones: metabolic actions in vitro. *Diabetologia* 45:1211–1223, 2002
48. Glass CK, Rosenfeld MG: The coregulator exchange in transcriptional functions of nuclear receptors. *Genes Dev* 14:121–141, 2000
49. Ge K, Guermah M, Yuan CX, Ito M, Wallberg AE, Spiegelman BM, Roeder RG: Transcription coactivator TRAP220 is required for PPAR gamma 2-stimulated adipogenesis. *Nature* 417:563–567, 2002
50. Knouff C, Auwerx J: Peroxisome proliferator-activated receptor-gamma calls for activation in moderation: lessons from genetics and pharmacology. *Endocr Rev* 25:899–918, 2004
51. Hallakou S, Doare L, Foufelle F, Kergoat M, Guerre-Millo M, Berthault MF, Dugail I, Morin J, Auwerx J, Ferre P: Pioglitazone induces in vivo adipocyte differentiation in the obese Zucker fa/fa rat. *Diabetes* 46:1393–1399, 1997
52. Boden G: Interaction between free fatty acids and glucose metabolism. *Curr Opin Clin Nutr Metab Care* 5:545–549, 2002